RSC Pharmaceutics

ROYAL SOCIETY OF CHEMISTRY

PAPER

View Article Online
View Journal | View Issue

Cite this: *RSC Pharm.*, 2025, **2**, 292

Drug-loaded 3D-printed magnetically guided pills for biomedical applications

Eirini Myrovali, *[a,b] Aikaterini-Theodora Chatzitaki,[b,c] Kyrillos Papadopoulos[a] and Dimitrios G. Fatouros[b,c]

The traditional treatment of stomach cancer is based on a combination of surgery and chemo/radiotherapy leading to severe side effects and endless pain. The objective of this study is the development of 3D-printed drug-loaded magnetic pills with multifunctional behavior under external stimuli to be exploited for cancer therapy in hollow organs. Their construction was based on magnetic hydrogels combined with doxorubicin. Firstly, the printing fidelity was examined using two ratios of sodium alginate to carbopol (1 : 2 and 2 : 1) with two different concentrations (4 and 8 mg mL^{-1}) of magnetic nanoparticles. The rheological measurements confirmed the material printability for preparing a 3D-printed magnetic pill in both ratios. The 3D-printed magnetic pill demonstrated strong magnetic attraction when subjected to an externally applied magnetic field confirming its ability to be remote-controlled. Thus, the magnetic component of the pills could be used for their locomotion in a targeted area using a static magnetic field, thereby increasing the residence time in a specific area of the stomach. All the prepared pills retained their morphology and shape confirming their structural integrity within a simulated gastric fluid solution (pH = 1.2). 3D-printed drug loaded magnetic and non magnetic pills were measured by applying an AC magnetic field with an amplitude of 50 mT and a frequency of 375 kHz to examine their heating ability and, consequently, the drug release. *In vitro* drug release from the 3D-printed drug-loaded magnetic pill has demonstrated a faster drug release (within 24 hours) compared with the non-magnetic 3D-printed pill. This enables a significantly localized drug release, on-demand, into the targeted area. The primary benefit of these applications could be the reduction in drug dosage, thereby potentially minimizing the immediate side effects associated with chemotherapy.

Received 3rd November 2024,
Accepted 2nd February 2025

DOI: 10.1039/d4pm00313f

rsc.li/RSCPharma

Introduction

Stomach cancer, also known as gastric cancer, is the third leading cause of morbidity and mortality worldwide. The forms of stomach cancer are plenty from a morphological perspective.[1] Although cancer is a serious condition, it can be curable with accurate diagnoses and effective treatments in its early stages.[2] Nowadays, 3D-printed materials could be used in terms of treating stomach cancer *via* oral administration. More researchers are paying attention to 3D printing technologies in the field of pharmaceutics due to their applicability to combine different materials with drugs to build objects from a 3D model.[3] The advantage of 3D concepts is the fact that they can be designed and printed within the same day in a very short time frame, whereas a conventional manufacturer would require several months to set up. 3D-printed drug loaded materials are extremely advantageous in terms of treating stomach cancer due to time-controlled release tablets, multi-active solid dosage forms and topical drug delivery.[4] However, the shortcomings with oral drugs are their rapid transit from the stomach to the small intestine and the cancellation of their structural integrity due to the low pH value (1–3.5) in the stomach.[5,6] Magnetic components in 3D-printed materials could be used to maintain the delivery system near their targeted zone and increase the residence time into a specific area of the stomach. On the other hand, natural or synthetic polymers could maintain the structural integrity of the drugs in low pH values. Thus, 3D-printed magnetic materials have emerged to address these challenges and play a significant role in the innovative fabrication of 3D smart materials for biomedical application.

Magnetic hydrogels, which are typically hydrogels in which magnetic nanoparticles (MNPs) are introduced, have attracted research interest for potential biomedical applications and 3D

[a]*School of Physics, Aristotle University of Thessaloniki, Thessaloniki, 54124, Greece. E-mail: emiroval@physics.auth.gr*
[b]*Department of Pharmaceutical Technology, School of Pharmacy, Aristotle University of Thessaloniki, GR-54124 Thessaloniki, Greece*
[c]*Center for Interdisciplinary Research and Innovation (CIRI-AUTH), Thessaloniki, Greece*

printing technology due to their magnetic actuation under an externally applied magnetic field.[7] The combination of MNPs with hydrogels could be used to prepare a smart magnetic material, which is responsive both to the magnetic field and the temperature. Consequently, the development of novel controllable release systems is of great significance. The range of potential applications of magnetic hydrogels is therefore extremely wide including soft actuators, environmental protection, chemical catalysis, engineering and biomedical applications.[8–10] Substantial research efforts are being currently devoted in terms of using magnetic hydrogels in biomedical applications, such as drug delivery. The magnetic response is more suitable for drug delivery than other stimuli, because of its remote operation, rapid reaction, and tunable manipulation.[11]

Another biomedical application where magnetic hydrogels can be used is magnetic particle hyperthermia for cancer treatment. Until now, this application usually uses a magnetic fluid containing magnetic nanoparticles to heat up the specific cancer organs or tissues to temperatures ranging between 41 and 45 °C.[12–14] In this temperature window, the malignant regions (*i.e.* cancer cells) undergo a severe thermal shock, while healthy tissues sustain this thermal regime with significantly milder side-effects. The use of magnetic hydrogels offers the advantage of preventing the leakage of MNPs, thereby reducing potential toxic effects in the surrounding area.[15,16]

The objective of this study is the development of a smart 3D-printed drug-loaded magnetic pill with multifunctional behavior under external stimuli to be exploited for stomach cancer therapy. The construction will be based on magnetic hydrogels combined with chemotherapy drugs. The hydrogel will act as a passive substrate for drug release, whereas the magnetic component will act as active element both for heating and magnetic actuation of the pill (locomotion) into a specifically targeted area, as presented in Fig. 1. The porosity of the hydrogels could function as an ideal platform for the encapsulation of drugs, while the drug delivery will be achieved by changing the temperature *via* heating produced by the magnetic nanoparticles during magnetic hyperthermia treatment. Therefore, the development of a 3D-printed drug-loaded pill, using magnetic hydrogels, is both promising and attractive at the same time. 3D printed magnetic hydrogels for oral drug delivery appear to be safe to use as they are excreted from the body after oral administration and there is no evidence of material accumulation in organs. Moreover, the magnetic component of the 3D printed pill could potentially control drug delivery to a specific area in the stomach and prolong gastric time without inducing severe side effects. Thus, the main advantage of such applications may be the minimization of both the drug dosage and the consequent side effects of the chemotherapy.

This work is focused on the synthesis of magnetic hydrogels, based on magnetite nanoparticles, and the preparation of 3D-printed magnetic pills loaded with drugs, such as doxorubicin (DOX), which are utilized in magnetic particle hyperthermia applications. Magnetite nanoparticles were exclusively used due to their excellent biocompatibility, tunable magnetic properties and their approval from Food and Drug Administration (FDA). The magnetite nanoparticles were synthesized using the chemical co-precipitation method. This method is a bottom-up, cost-effective, fast process that can be easily expanded to an industrial level.[17,18] Compared with other synthetic routes, the co-precipitation pathway is generally preferred due to its high yield, facile control, and very low-cost production.[19,20] Following the synthesis of MNPs, the printability of hydrogels was determined through rheological measurements using two different ratios of natural and synthetic hydrogels. This was an important step to establish the optimal conditions for creating a stable and printable 3D pill. The good magnetic response of a 3D-printed magnetic pill was evaluated using a static magnetic field under Simulated Gastric Fluid (SGF) solution with a pH value of 1.2. Ultimately, magnetic hyperthermia measurements were conducted at a frequency of 375 kHz and an alternating magnetic field of 50 mT using both drug-loaded magnetic and non-magnetic pills. The release of DOX from a drug-loaded magnetic pill was significantly increased when heated under magnetic hyperthermia conditions compared with a drug-loaded non-magnetic pill. Thus, 3D-printed magnetic pills could be characterized as a novel and cost-effective method characterized by faster symptom relief compared with other conventional treatments and will have potentially high scientific impact on biomedical applications for cancer therapy.

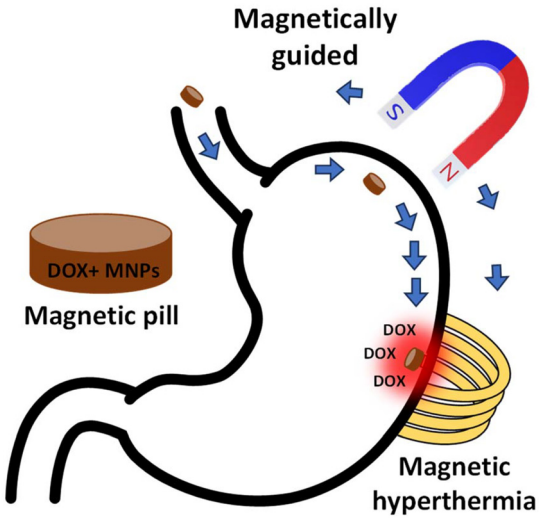

Fig. 1 The schematic illustrates a 3D-printed, drug-loaded magnetic pill (brown color pill), which functions as a magnetic actuator capable of moving under an externally applied magnetic field (magnetically guided pill). The 3D-printed drug-loaded magnetic pills are explored as smart materials due to the double action stimuli owning the ability to deliver drugs and release heat into a specific area through the application of magnetic hyperthermia within the therapeutic temperature range of 41–45 °C.

Materials and methods

Materials

Carbopol 940 and calcium chloride were purchased from Lubrizol (Brussels, Belgium) and FerakLaborat GMBH (Berlin, Germany), respectively. Alginate acid sodium salt and doxorubicin hydrochloride (98.0–102.0% HPLC) were supplied by Sigma-Aldrich Co Ltd (Darmstadt, Germany). Milli-Q water was of analytical grade.

Synthesis of MNPs

Magnetite nanoparticles were synthesized using the oxidative aqueous co-precipitation method with iron salts adhering to a standard procedure detailed in prior studies.[21,22] The size of the nanoparticles was regulated by the concentration of sodium hydroxide (NaOH). Initially, a solution of sodium nitrate $NaNO_3$ (0.2 M) was combined with equal parts of ethanol and water, referred to as solution A henceforth. Subsequently, a blend of iron(II) sulfate heptahydrate $FeSO_4{\cdot}7H_2O$ (0.2 M) and sulfuric acid H_2SO_4 (0.01 M) was introduced to solution A and stirred vigorously. Concurrently, a NaOH (0.4 M) solution was incrementally added to maintain the desired pH value (pH = 10). The resultant mixture was then heated to 90 °C and maintained for three hours. Afterward, it was allowed to cool to room temperature. The solid particles were finally isolated through magnetic decantation and repeatedly rinsed with distilled water.

Characterization of MNPs

The crystal structure of the MNPs was identified by X-ray diffraction (XRD) using a two-cycle Rigaku Ultima Plus X-ray diffractometer with a Cu-Kα (λ = 1.5406 Å) radiation operating at 40 kV and 30 mA. The increment of 2θ angle was kept constant at 0.05°, while data acquisition dwell time was set 3 s in Bragg-Brentanogeometry. To investigate the morphology, microstructure and the size distribution of the MNPs, samples for transmission electron microscopy (TEM) were prepared by drop-casting the colloidal dispersions onto carbon-coated Cu grids after sonication for 1 h in water. TEM and high-resolution TEM (HRTEM) were performed by a JEOL 2011 UHR microscope with a 0.194 nm point resolution operated at 200 kV. Magnetic hysteresis loops (major loops at ±1 T) were recorded at 300 K using vibrating sample magnetometry (VSM) in a Quantum Design Dynacool PPMS system.

Magnetic particle hyperthermia

An induction heating setup system is used for magnetic heating operating at 375 kHz (2.4 kW Easyheat/Ambrell). The amplitude of the magnetic field was 50 mT. The temperature was recorded by using a GaAs-based optical fiber probe and thermal imaging camera (FLIR). Each measurement cycle included a heating and a cooling stage.

3D printing procedure

Hydrogels without any bubbles were printed using the semi-solid extrusion (SSE) 3D printing method (Inkredible 3D bioprinter, Cellink, Gothenburg, Sweden). Pill shaped objects were designed in Autocad 2019 (Autodesk Inc., CA, USA) with a diameter of 6 mm and a height of 2 mm, whereas the printing nozzle was 25 G – 0.26 mm diameter. The printing speed was set at 8 mm s^{-1} and the infill was 100% with concentric pattern. The printing process was conducted on pre-weight plates and the weight of the final 3D-printed object was determined by the difference between the weight of the plate before and direct after printing. To facilitate easy handling of the 3D-printed hydrogel, the final 3D-printed objects were cross-linked with $CaCl_2$ for 15 minutes and the salt residues were washed with distilled water. The cross-linked structures were stored in 2 mL Milli-Q water overnight before further assays.

Rheological characterization

The rheological properties of freshly prepared blank inks were carried out using an MCR 302 rheometer (Anton Paar, Graz, Austria) with the parallel plate geometry (diameter 25 mm) at a gap of 1 mm and 25 °C. Viscosity test was measured as a function of shear rate at shear rates 0.1–100 1 s^{-1}. Frequency oscillatory sweep tests were performed at strain value of 1% and at a frequency range of 1 to 100 Hz.

Encapsulation efficiency

The amount of the entrapped DOX was determined with indirect method. In particular, the released DOX in Milli-Q water after overnight storage at 4 °C was analyzed using the fluorescent method. The fluorescence of DOX was measured using excitation and emission wavelengths of 488 and 590 nm, respectively, and slit excitation 5 and emission 10 with a standard calibration curve in Milli-Q water (0.0125–0.0625 ppm, R^2 = 0.999).

In vitro release

The *in vitro* release profile of the 3D-printed hydrogels was examined in SGF (pH 1.2). 3D-printed pills were immersed in 1 mL SGF and remained for 10 minutes in magnetic hyperthermia conditions. After this period, 4 mL SGF were added in the same falcon and this time point was set as t = 0. Falcons remained in a shaking bath at 70 rpm at 37 ± 0.2 °C and 1 mL aliquots was withdrawn at specific time points from the starting point (t = 0) up to day 9 followed by replacement with fresh pre-heated SGF. The analysis of DOX was performed as outlined previously using standard calibration curves in SGF at concentration range of 0.0125–0.0625 ppm (R^2 = 0.999).

Statistical analysis

The data are expressed as the mean ± standard deviation (SD) based on at least three measurements. Statistical analysis was performed using a t-test, with differences considered significant at $P \leq 0.05$.

Results and discussion

Structural and magnetic properties

The morphological and structural characteristics of the MNPs at the nanoscale are depicted in Fig. 2a. The TEM image

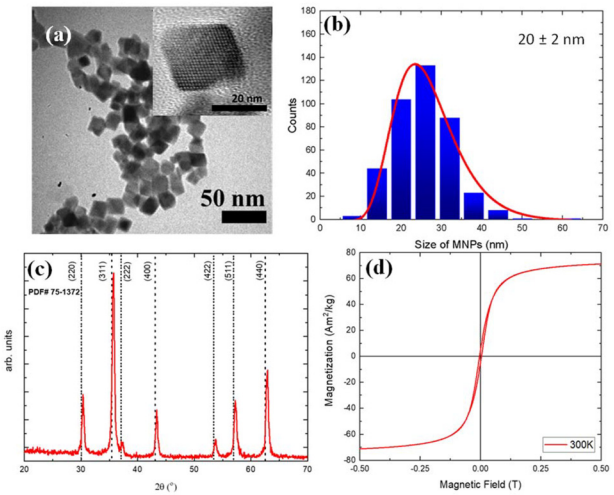

Fig. 2 (a) Representative TEM image of magnetite MNPs accompanied by an HRTEM image (inset) of the single particle. (b) Size distribution of the MNPs (20 ± 2 nm). (c) X-ray diffraction pattern of magnetite NPs. (d) Hysteresis loop within a DC magnetic field of ±0.5 T at RT (300 K).

(Fig. 2a) reveals that the MNPs possess a faceted, cubic-like morphology with distinct edges. Additionally, the corresponding HRTEM image (inset Fig. 2a) confirms the high crystallinity of the sample due to the clear lattice boundary. The average size of the MNPs was determined to be 20 ± 2 nm, which was calculated by using log–normal distribution fitting, as illustrated in Fig. 2b. The X-ray diffraction pattern, as depicted in Fig. 2c, reveals that the diffraction peaks of the MNPs are consistent with the magnetite standard reference card (PDF#751372#). The hysteresis loops were recorded at room temperature (RT), as shown in Fig. 2d. The saturation magnetization reached 73 Am^2 kg^{-1} at 1 T, which aligns well with findings from relevant studies.[23–25] Consequently, the properties demonstrated by the MNPs render them ideal candidates for the creation of 3D-printed magnetic pills.

3D printing process optimization

Three-dimensional (3D) printing is considered an emerging digital technology that could combine different materials to construct objects from a 3D model, which could be utilized as a key driving factor for the future advancement and precise manufacturing of personalized dosage forms, regenerative medicine, prostheses, and implantable medical devices.[26,27] Printing hydrogels into a 3D construction is a very challenging process. There are natural polymers with good biocompatibility and low immunogenicity, such as chitosan, gelatin methacrylate (GelMa), gelatin, collagen, as well as synthetic polymers with low printability.[28–31] However, the combination of natural and synthetic hydrogels can modify the network ratio to prepare a printable material.[32] Sodium alginate, a prevalent natural polymer, is increasingly significant in the healthcare and pharmaceutical industries due to biocompatibility, biodegradability, versatility, sustainability and functionalization for drug delivery.[33] It serves as an effective matrix for cell immobilization and entrapment of bioactive substances and pharmaceuticals.[34] Materials encapsulated within the inert alginate matrix can be administered at a controlled rate using a controlled release system.[35] Drugs encapsulated within alginate beads are discharged through diffusion *via* pores and this release is expedited by the breakdown of the alginate polymer network.[36] On the other hand, carbopol is widely recognized as a synthetic polymer with superior physical and rheological properties.[37] Carbopol is widely recognized for its mucoadhesive properties, which facilitate targeted drug delivery to specific absorption sites. It is also commonly used in oral formulations to provide sustained drug release, thereby maintaining therapeutic drug levels over a prolonged period and enhancing overall efficacy.[38,39] Nowadays, magnetic hydrogels have drawn research attention for potential biomedical applications due to magnetic actuation under an externally applied magnetic field.[40] The range of potential applications of magnetic hydrogels is therefore extremely wide including soft actuators, environmental protection, chemical catalysis and engineering, as well as biomedical applications. Substantial research efforts are being currently devoted to use magnetic hydrogels in biomedical applications, such as drug delivery. The key to develop smart drug-loaded hydrogels, which react upon an external stimulus, is the incorporation of multifunctional materials. The magnetic response is more suitable for drug delivery than other stimuli, because of its remote operation, rapid reaction and tunable manipulation.[41] Consequently, different ratios of sodium alginate to carbopol were mixed with magnetic MNPs and drug to create a consistent and an extrudable ink of magnetic hydrogel.

Development of drug-loaded magnetic inks

Two ratios of sodium alginate to carbopol, 1 : 2 and 2 : 1, were evaluated for their printing fidelity. Initially, sodium alginate and carbopol powders were dispersed in distilled water (Milli-Q) and mixed thoroughly, as depicted in Fig. 3a. The resulting solution of non-magnetic ink is presented in Fig. 3b. Following this procedure, two pathways emerge for the preparation of drug-loaded inks: (a) non-magnetic ink and (b) magnetic ink, as illustrated in Fig. 3b. Drug-loaded non-magnetic ink was fabricated by incorporating a solution of DOX into the non-magnetic ink (Fig. 3c). Conversely, drug-loaded magnetic ink was prepared by combining solutions of magnetic nanoparticles and DOX (Fig. 3d). All solutions were vigorously mixed to create a homogeneous printing solution and then stored at 4 °C for 15 minutes to ensure complete hydration of the polymers. Finally, each solution was drawn into a syringe to create various inks for the 3D printer. It is important to mention that DOX powder was dissolved in distilled water, while the final concentration of DOX remained constant at 0.05 mg mL^{-1} in both cases. DOX was used because it is a widely utilized medication for treating various forms of cancer.[42,43] Prior to incorporating the MNPs into the non-magnetic ink, the MNPs were first dispersed in distilled water and subsequently sonicated to ensure their homogeneous distribution. Additionally, the MNPs were evaluated at the concen-

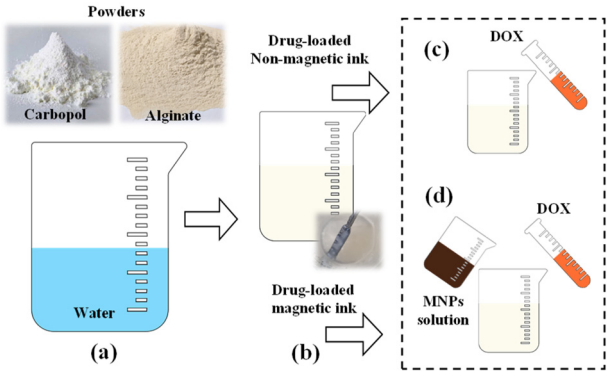

Fig. 3 Schematic illustrations of inks: (a) dispersion of powders (carbopol and alginate) in distilled water and the formulation of (b) non-magnetic ink; (c) drug-loaded non-magnetic ink; and (d) drug-loaded magnetic ink.

trations of 4 and 8 mg mL^{-1} to determine the most effective heating performance in magnetic hyperthermia. Previous research on magnetic polymers has demonstrated that there is no leakage of iron oxide NPs into the water solution, even by increasing the MNPs concentration from 1 to 8 mg mL^{-1}.[44] These findings suggest that magnetic inks can be utilized in subsequent experiments and in biomedical applications at elevated concentrations up to 8 mg mL^{-1}.

Rheological characterization of magnetic inks

Optimal inks must possess two key characteristics: firstly, they should demonstrate shear-thinning behavior when a deforming force is applied; and secondly, their viscosity should rapidly increase once the force is removed to ensure high shape fidelity and precise printing.[45,46] Viscosity and viscoelastic shear modulus are crucial rheological parameters for understanding the flow behavior of combined hydrogels. Viscosity is the measure of a fluid's resistance to flow when stress is applied, significantly affecting extrudability, printing precision, as well as the maintenance of shape.[47]

The viscosity as a function of shear rate is shown in Fig. 4a for both ratios of the polymers. According to Fig. 4a, the viscosity is higher in the polymer with the ratio of 2 : 1 (blue color) than the ratio of 1 : 2 (black color). This behavior implies that a lower ratio (1 : 2) could result in greater printing precision and better shape retention post-extrusion, compared with the higher ratio (2 : 1). This could be attributed to the higher amount of carbopol, which has been characterized as an agent that modifies rheological properties of pastes, thereby enhancing the fidelity of 3D-printed structures.[48] However, at higher shear rates, the values become equal indicating a consistent viscosity throughout the printing process. Additionally, both ratios of inks demonstrated shear-thinning behavior, evident from the reduction in viscosity as the shear rate increased, which is a common trait of polymeric formulations.[49] It should be noted that prior research indicated that a viscosity exceeding 300 mPa·s results in an irreversible shape during 3D printing.[50] Regarding viscosity measurements, both

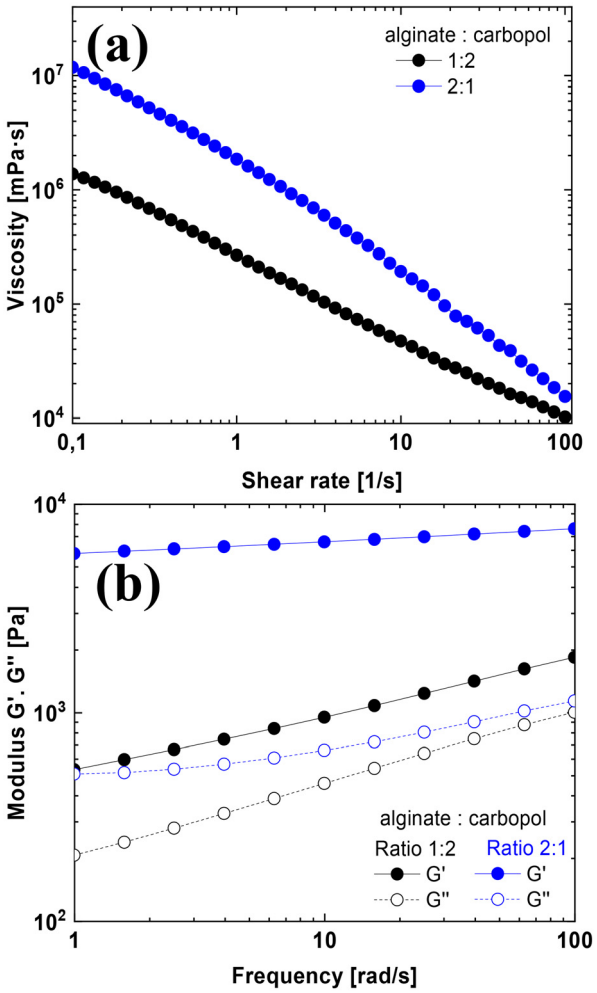

Fig. 4 Rheological analysis of freshly prepared inks using two different ratios of sodium alginate to carbopol, 1 : 2 (black) and 2 : 1 (blue), respectively. (a) Viscosity measurements at shear rates 0.1–100 1 s^{-1}, (b) mechanical strength of inks using storage (G') and loss (G'') modulus of frequency sweep test at a strain value of 1% within the frequency range of 1 to 100 Hz.

ratios are suitable for the formulation of 3D-printed magnetic pills.

Additionally, the mechanical strength of inks could reveal significant insights into the material printability. The mechanical strength of inks was assessed using a frequency sweep oscillatory test, as depicted in Fig. 4b. In rheology, G' denotes the energy stored and recovered in each deformation cycle. Essentially, it acts as a catalyst for the restructuring of a material after undergoing deformation due to applied stress. On the other hand, G'' measures the energy dissipated per cycle, indicative of the liquid-like behavior of the material. In both cases, the storage modulus (G') of all printable inks exhibited a higher magnitude than the loss modulus (G'') as shown in Fig. 3b with solid and open symbols, respectively. Both inks displaying elastic behavior and a (G') value exceeding 500 Pa have shown sufficient structural support after deposition.[51,52] Consequently, the rheological properties of

alginate/carbopol hydrogel ratios were assessed and demonstrated to be highly promising for the development of 3D-printed magnetic pills.

3D-printed pill formation and magnetic actuation within SGF

The prepared inks (Fig. 5a) were utilized to fabricate pills with a maximum height of 2 mm and a maximum diameter of 6 mm using a 3D printer, as depicted in Fig. 5b. Three variants of 3D-printed pills were produced: (a) non-magnetic, (b) drug-loaded non-magnetic and (c) drug-loaded magnetic, presented in Fig. 5c, d, and e, respectively. Previous study has shown that crosslinking, such as calcium chloride ($CaCl_2$), is an important parameter in the fabrication of polymers that can result in enhanced stability by developing inter-molecular network linkages.[53] Indeed, following their preparation, the pills were immersed in a $CaCl_2$ solution to enhance their stability and shape retention.

Moreover, to assess the magnetic behavior of the synthesized drug-loaded magnetic pill, a commercial NdFeB magnet was placed adjacent to the test tube, showcasing the magnetic response of the pill, as illustrated in Fig. 5f. The magnetic pill could be characterized as suitable for drug delivery due to remote operation, rapid reaction and tunable manipulation. Next step is to examine the behavior of the pills within gastric conditions. In healthy humans, the pH level of gastric fluid typically ranges from approximately 1 to 2 indicating an acidic environment.[54] Consequently, the pills were placed into a SGF solution owning a pH value of 1.2 to probe the structural integrity of the pills at 37 ± 0.2 °C. Both pill ratios preserved their perfect shape after 24 hours of exposure in the SGF solution (Fig. 5g). These results indicate that the MNPs could be stable within the polymer matrix, which was not dissolved in gastric fluids. Indeed, there is no leakage of MNPs in SGF solution after 24 hours in both ratios (Fig. 5h, ratio 1 : 2). These findings suggest that the magnetic pills could be the perfect candidate for drug delivery on-demand into specific area.

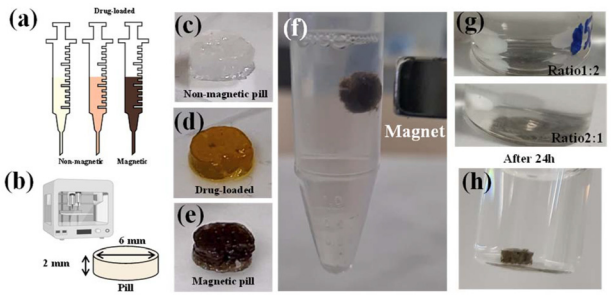

Fig. 5 (a) Schematic representation of syringes filled with different inks and (b) illustration of pill with a maximum height of 2 mm and a maximum diameter of 6 mm using a 3D printer. 3D-printed pills before $CaCl_2$ bath: (c) non-magnetic, (d) drug-loaded non-magnetic, and (e) drug-loaded magnetic. (f) Picture of magnetic-pill responding to an externally applied magnetic field (magnet). (g) Two pill ratios, 1 : 2 and 2 : 1, reflecting the shape integrity after 24 hours of exposure in the SGF solution at 37 ± 0.2 °C. (h) No leakage of MNPs using a magnetic pill (with ratio 1 : 2) in SGF solution at 37 ± 0.2 °C for 24 hours.

Heating efficiency of magnetic particle hyperthermia

The study of the magnetically induced heating efficiency encompassed assessments of a magnetic pill with a MNPs concentration of 8 mg mL^{-1} (Fig. 6a), as well as a non-magnetic pill (Fig. 6b) with a 1 : 2 alginate to carbopol ratio. Both of them were subjected to an alternating (AC) magnetic field of 50 mT and a frequency of 375 kHz, whereas each sample was placed at the coil's center (Fig. 6a and b). Initially, the temperature was recorded using a thermal camera during the measurement, which was positioned above the coil (Fig. 6c).

Thermal imaging confirmed that the temperature of the magnetic pill increased from 28.3 °C to 44.7 °C, as shown in Fig. 6d, resulting in a color change from purple to yellow. The same thermal behavior was presented in the magnetic pill with a MNPs concentration of 4 mg mL^{-1} increasing the duration of hyperthermia measurement. One the other hand, the temperature of the non-magnetic pill varied between 25.1 °C and 29.2 °C maintaining its purple color throughout the hyperthermia measurement, as depicted in Fig. 6e. The significant temperature disparity between the two samples can be attributed to the ferromagnetic properties of the MNPs. Ferromagnetic particles possess the ability to heat up when subjected to an AC magnetic field due to magnetic hysteresis losses.[20]

Following the confirmation of the heating capabilities of the magnetic pills, the subsequent crucial step involved the assessment of the samples in a SGF to mimic the condition of the stomach. For this purpose, pills containing two distinct

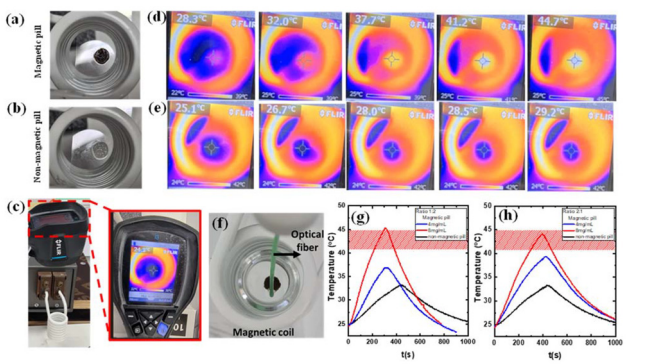

Fig. 6 (a) Magnetic pill and (b) non-magnetic pill placed in the center of the coil. (c) Thermal camera above the coil. Dash red line: thermal image without sample when applying a magnetic field. Thermal images during hyperthermia measurement by applying an AC field of 50 mT and a frequency of 375 kHz in (d) magnetic and (e) non-magnetic pill. The color bar of each image indicates the local temperature. (f) Magnetic pill in SGF within a magnetic coil recording the temperature using an optical fiber (green color). Hyperthermia curves of magnetic measurements at 375 kHz/50 mT using magnetic and non-magnetic pills with alginate to carbopol ratio of (g) 1 : 2 and (h) 2 : 1. The hyperthermia measurements were taken using non-magnetic pill (black color) and magnetic pill with MNPs concentration of 4 and 8 mg mL^{-1} (red and blue color).

ratios of alginate to carbopol and two different concentrations of MNPs were utilized. A single pill was submerged in a container with 1 mL of SGF, positioned at the coil's center and its temperature was monitored using an optical fiber, as depicted in Fig. 6f. The hyperthermia curves of the magnetic pill and the non-magnetic pill, with alginate to carbopol ratios of 1 : 2 and 2 : 1, are depicted in Fig. 6g and h, respectively. Starting with the heating curve of the pills with an alginate to carbopol ratio of 1 : 2, the magnetic pill with a MNPs concentration of 8 mg mL^{-1} quickly reached the hyperthermia window of 41–45 °C (indicated by the red frame in Fig. 6g). Specifically, the sample reached a peak temperature of 45.2 °C after 300 seconds of exposure, as shown by the red line in Fig. 6g. On the contrary, the magnetic pill with the lower MNPs concentration of 4 mg mL^{-1} did not reach the hyperthermia window within the same exposure duration. Pills with a 2 : 1 alginate to carbopol ratio exhibited similar thermal behavior. Specifically, the magnetic pill achieved a maximum temperature of 44.9 °C after 400 seconds of exposure, indicated by the red line in Fig. 6h, while the magnetic pill with a lower MNPs concentration did not reach the hyperthermia threshold within the same timeframe, as depicted by the blue line in Fig. 6h. In both cases of lower MNPs concentration (4 mg mL^{-1}), the results suggest that a longer exposure duration was required to reach the hyperthermia window. It is important to mention that the non-magnetic pill displayed consistent thermal behavior at both ratios and remained below the hyperthermia threshold, with the highest recorded temperature being 33 °C. Nonetheless, the magnetic pills with a lower concentration of MNPs (4 mg mL^{-1}) exhibited higher temperatures compared with the non-magnetic pills in both ratios, as demonstrated in Fig. 6g and h, thereby confirming the heating capability of the MNPs. The results indicated a strong correlation between the heating rate of the magnetic pill and the MNPs concentration. A higher concentration of MNPs resulted in an increased heating rate and reduced the required exposure duration. On the basis of these results, the higher concentration of MNPs (8 mg mL^{-1}) was selected in both cases of ratios for studying the drug release within an AC magnetic field.

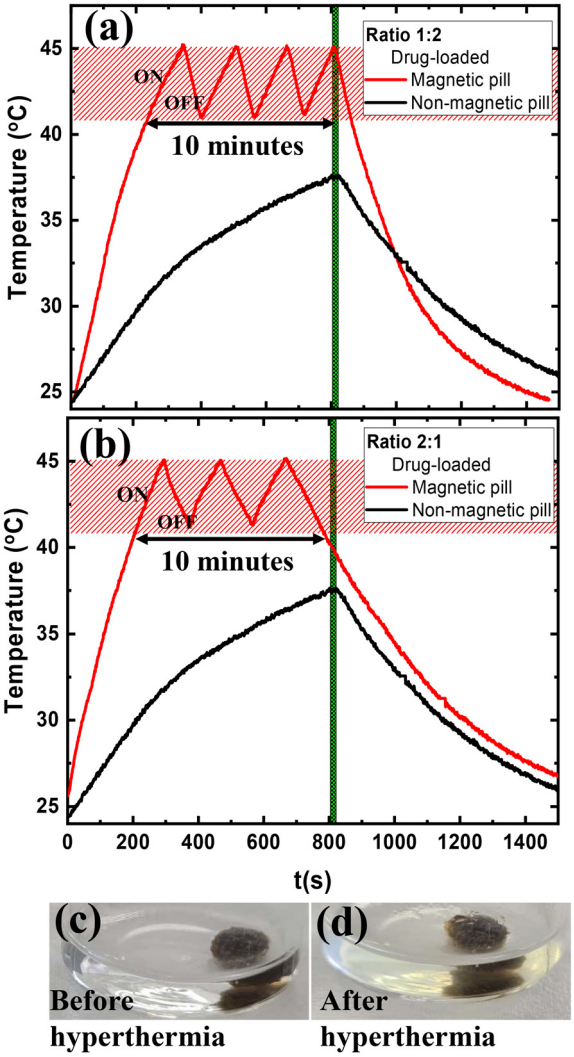

Fig. 7 Hyperthermia curves of magnetic measurements at 375 kHz/50 mT using drug-loaded magnetic and non-magnetic pills with an alginate to carbopol ratio of (a) 1 : 2 and (b) 2 : 1. (c) and (d) Optical images of drug-loaded magnetic pills before and after hyperthermia experiment, respectively.

Drug release on-demand

The next step is to study the drug-loaded magnetic pill in hyperthermia conditions at 375 kHz and 50 mT in SGF solution using both ratios. To maintain the pill within the hyperthermia threshold (marked by the red frame in Fig. 7) for 10 minutes, an "on–off" heating pattern was created by alternating the AC magnetic field between ON and OFF states. The AC magnetic field was deactivated to allow cooling to 41 °C and it was reactivated to heat the pill up to 45 °C. The magnetically induced heating capability of the MNPs allows the magnetic pills to be remotely controlled for drug release on-demand.

Fig. 7a and b displayed drug-loaded magnetic pills with alginate to carbopol ratios of 1 : 2 and 2 : 1, respectively. The AC magnetic field was activated four times in 10 minutes for the 1 : 2 ratio and three times for the 2 : 1 ratio. This behavior could be explained *via* viscoelastic properties. The viscosity in the polymer matrix ratio of 1 : 2 is lower than that of the 2 : 1 ratio (Fig. 4a). That means the MNPs can rotate more quickly in the polymer matrix ratio of 1 : 2 than 2 : 1 leading to a faster thermal response. This behavior is in good agreement with another study, which has shown that the augmented mobility of the MNPs in the medium, *i.e.* Brownian relaxation due to the physical rotation of the particles, could increase their heating response.[22] Conversely, the non-magnetic pill failed to reach the hyperthermia threshold even after 800 seconds (Fig. 7a and b, black color).

During the measurements, optical images were taken before and after hyperthermia to examine the drug release into the SGF solution, as shown in Fig. 7c and d for the drug-loaded magnetic pill with a MNPs concentration of 8 mg mL^{-1}

and an alginate to carbopol ratio of 1 : 2. The same behavior was demonstrated by the drug-loaded magnetic pill with a MNPs concentration of 8 mg mL^{-1} and an alginate to carbopol ratio of 2 : 1. Optical images confirm the drug release deriving from the magnetic pills, which enables the triggered release of drugs into the SFG solution after magnetic hyperthermia. These results demonstrate that drug-loaded magnetic pills may be explored as a potential method for remotely controlled drug delivery to targeted areas using magnetic hyperthermia treatment.

In vitro drug release from drug-loaded pills by time

The *in vitro* release profiles of DOX were examined at different intervals (0, 24, 48, 72, 144 and 216 hours) at 37 ± 0.2 °C to demonstrate the efficacy of both drug-loaded magnetic pills and drug-loaded non-magnetic pills for triggered drug release in SGF solution with a pH value of 1.2, with and without magnetic hyperthermia treatment. All measurements were conducted for alginate to carbopol ratios of 1 : 2 and 2 : 1, as shown in Fig. 8a and b, respectively. Drug loaded magnetic pill (blue spheres) and non-magnetic pill (red spheres) referred to the drug release which occurred at 0, 24, 48, 72, 144 and 216 hours after the magnetic hyperthermia treatment, while drug loaded magnetic pills referred to the drug release from 0 to 216 hours without magnetic hyperthermia treatment (black spheres).

DOX release from magnetic pill (blue color) was significantly enhanced by heating after the magnetic hyperthermia treatment compared with the control experiments (non-magnetic pill after hyperthermia treatment and magnetic pill without hyperthermia treatment) performed at 37 ± 0.2 °C in both ratios, as shown in Fig. 8a and b. For the non-magnetic pill, the drug release ranged from 7% to 68% and from 4.5% to 58% for the ratios of 1 : 2 and 2 : 1, respectively, over a period of 216 hours after the hyperthermia treatment (Fig. 8, red color). Similar drug release behaviour was observed in the drug loaded magnetic pill without hyperthermia treatment. Specifically, the drug release ranged from 3.7% to 72% and from 3.7% to 63% for the ratios of 1 : 2 and 2 : 1, respectively, over a period of 216 hours, as shown in Fig. 8 in black color. These results indicate that the magnetic pill without hyperthermia and non-magnetic pills after hyperthermia have the same drug release behavior over time. On the contrary, the drug-loaded magnetic pills after hyperthermia treatment can increase the release of DOX from 18.5 to 78% and 20 to 68%, after 24 hours, for the ratios of 1 : 2 and 2 : 1, respectively (Fig. 8, blue color). After 24 hours, the drug release values kept constant over time in both ratios. That means the drug release was achieved very quickly (24 hours) in magnetic pills after hyperthermia treatment (blue color) compared with the drug release observed without magnetic hyperthermia treatment (black color) in 216 hours. These data indicated that the magnetic pills under study could serve as a platform for on-demand drug delivery within 24 hours. This potential enhancement in diffusive release could be particularly beneficial for drugs that are more challenging to administer.

However, it is important to mention that the different carbopol to alginate ratio could affect the drug release. Indeed, the drug release is better in the ratio of 1 : 2 than that in the ratio of 2 : 1 in all pills, as shown in Fig. 8a and b. This phenomenon demonstrated that the porous density of the 1 : 2 ratio was greater than that of the 2 : 1 ratio. Consequently, the increased porosity resulted in the greater release of the drug. To visualize the drug release, optical images were taken in non-magnetic pills using both ratios. The optical images depicting the time-dependent release response of DOX at 37 ± 0.2 °C from a non-magnetic pill are illustrated in Fig. 8c and d for the ratios of 1 : 2 and 2 : 1, respectively. The drug release is signified by the color change in the non-magnetic pill. The results indicated that the drug release was highest at the ratio of 1 : 2 compared with the ratio of 2 : 1. Indeed, factors such as the concentration of inks, crosslinking density, as well as content of MNPs in the matrix of hydrogel can reduce the release of the drugs.[55–57] As a result, the drug release cannot reach the maximum value of 100%. The results confirmed that the porosity of the hydrogels functioned as a platform for encapsulating drugs, while the drug delivery achieved by changing the temperature *via* the heating produced by magnetic nanoparticles within AC magnetic fields. This study has verified that the application of magnetic hyperthermia significantly boosts the release of DOX, thereby enabling a considerably localized drug discharge in the region subjected to the magnetic field.

Considering all the data above, the 3D-printed drug loaded magnetic pills could be a strategy to enhance the oral drug delivery. The challenge is to select the 3D-printed pill, which is

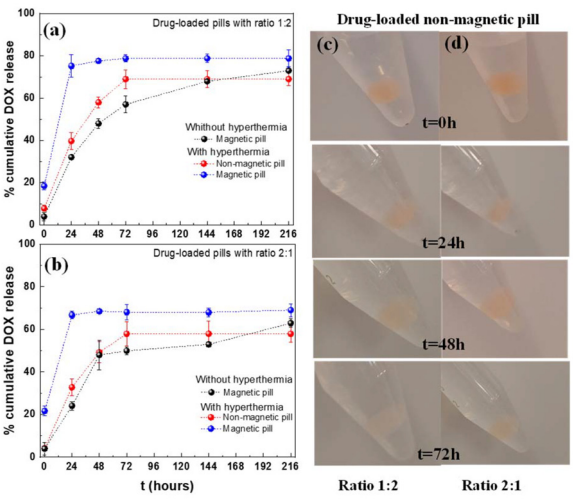

Fig. 8 *In vitro* release of DOX from a drug-loaded magnetic pill with and without hyperthermia treatment (blue and black spheres), as well as from a drug-loaded non-magnetic pill following hyperthermia measurements (red spheres) using an alginate to carbopol ratio of (a) 1 : 2 and (b) 2 : 1. All measurements were taken in SGF solution at 37 ± 0.2 °C. Optical images of time-dependent release response of DOX at 37 ± 0.2 °C from a non-magnetic pill for ratios (c) 1 : 2 and (d) 2 : 1. The *in vitro* release profiles of DOX were examined at different intervals (0, 24, 48, 72, 144 and 216 hours).

most suitable for each patient and the type of pharmaceutical ink that should be developed possessing the required drug dosage to treat stomach cancer. Personalized medicine takes a step forward by combining magnetic hydrogels and 3D-printing techniques. 3D-printed drug-loaded magnetic pills could be prepared for oral administration for each patient. An external magnetic field can be employed to direct the magnetic pill to a targeted area increasing its residence time in the stomach. Owing to their nature, hydrogels could maintain their structural integrity in acidic media. The external magnetic field could be utilized until the maximum drug release will be achieved.3D-printed pills will be explored as smart materials due to the double action stimuli owning the ability to deliver drugs and release heat into a specific area through the application of magnetic particle hyperthermia within the therapeutic temperature range of 41–45 °C. Moreover, the magnetic component of a 3D-printed pill potentially controls drug delivery to a specific area in the stomach and prolongs retention time without inducing severe side effects. The multi action stimuli based on 3D-printed pills could be utilized as a multifunctional platform to cure cancer in hollow organs, such as stomach. Thus, 3D-printed drug-loaded pills will have potentially high scientific impact on clinical applications.

Conclusions

In summary, magnetite nanoparticles were synthesized using the co-precipitation method, an eco-friendly technique with straightforward synthetic control. XRD patterns, TEM and HRTEM images confirmed that the MNPs are single-crystalline magnetite nanoparticles with a typical size of 20 ± 2 nm and cubic-like morphology. Two ratios of sodium alginate to carbopol, 1 : 2 and 2 : 1, were combined with MNPs in two different concentrations (4 and 8 mg mL^{-1}) to assess their printing fidelity. Rheological properties of inks confirmed material printability for preparing a 3D-printed magnetic and non-magnetic pill at two different ratios of alginate to carbopol. Magnetic pills have demonstrated strong magnetic attraction when subjected to an externally applied magnetic field. This indicates that these pills can be remotely controlled by a static magnetic field. Additionally, the magnetic and non-magnetic pills were placed into a SGF solution mimicking the condition inside of the stomach, with a pH value of 1.2 and a temperature of 37 ± 0.2 °C for 24 hours. All the pills retained their morphology and shape confirming their structural integrity. Measurements of magnetic hyperthermia were conducted on both magnetic and non-magnetic pills by applying an AC magnetic field of 375 kHz/50 mT. The findings revealed a significant correlation between the heating rate of the magnetic pill and the concentration of the MNPs. Consequently, the higher MNPs concentration (8 mg mL^{-1}) resulted in an increased heating rate, while the non-magnetic pill did not manage to reach the hyperthermia threshold. This behavior was also confirmed by thermal images obtained during the magnetic hyperthermia measurements. Maintaining a higher MNPs concentration of 8 mg mL^{-1}, hyperthermia measurements indicated that the heating performance of the magnetic pill with an alginate to carbopol ratio of 1 : 2 was superior to that of the 2 : 1 ratio owing to the reduced viscosity. MNPs can rotate more quickly in the polymer matrix ratio of 1 : 2 than 2 : 1 resulting in a faster thermal response. *In vitro* drug release in the 3D-printed drug-loaded magnetic pill has demonstrated a quicker drug release compared with the non-magnetic 3D-printed pill. This allows for a significant localized drug release on-demand in the targeted area.

The ability to control the drug release into a specific area, as a function of the AC magnetic field, will give the opportunity to reduce the total dose of the drugs and the consequent side effects of the chemotherapy. The new generation of 3D-printed magnetic pills is being investigated as smart materials, because of their dual-action stimuli. They have the capability to deliver medication and generate heat in a targeted area through magnetic particle hyperthermia within the therapeutic temperature range of 41–45 °C. Furthermore, the magnetic aspect of the pill can facilitate its locomotion to a specific area by using a static magnetic field (DC field). This approach could improve the possibility of tumor overgrowth, thus treating advanced unresectable cancer. Smart 3D-printed pills could be used as a novel and cost-effective method with faster symptom relief compared with other conventional treatments.

Data availability

All data that support the findings of this study are included within the article.

Conflicts of interest

There are no conflicts to declare.

Acknowledgements

We would like to thank Professor Makis Angelakeris from the School of Physics at the Aristotle University of Thessaloniki for providing the magnetic hyperthermia device and Professor Ulf Wiedwald from the University of Duisburg-Essen, Germany, for providing the equipment to collect magnetic data and structural images.

References

1 E. C. Smyth, M. Nilsson, H. I. Grabsch and N. C. Van Grieken, Gastric cancer, *Lancet*, 2020, **396**, 635–648.
2 K. Osawa, R. Nakadate, J. Arata, Y. Nagao, T. Akahoshi, M. Eto and M. Hashizume, Self-propelled colonoscopy robot using flexible paddles, *IEEE Robot. Autom. Lett.*, 2020, **5**(4), 6710–6716.

3 J. Capel, R. P. Rimington, M. P. Lewis and S. D. R. Christie, 3D printing for chemical, pharmaceutical and biological applications, *Nat. Rev. Chem.*, 2018, **2**(12), 422–436.
4 R. C. R. Beck, P. S. Chaves, A. Goyanes, B. Vukosavljevic, A. Buanz, M. Windbergs, A. W. Basit and S. Gaisford, 3D printed tablets loaded with polymeric nanocapsules: An innovative approach to produce customized drug delivery systems, *Int. J. Pharm.*, 2017, **528**(1–2), 268–279.
5 S. S. Davis, Formulation strategies for absorption windows, *Drug Discovery Today*, 2005, **10**(4), 249–257.
6 T. Yoshida, T. C. Lai, G. S. Kwon and K. Sako, pH-and ion-sensitive polymers for drug delivery, *Expert Opin. Drug Delivery*, 2013, **10**(11), 1497–1513.
7 B. Sun, R. Jia, H. Yang, X. Chen, K. Tan, Q. Deng and J. Tang, Magnetic Arthropod Millirobots Fabricated by 3D–Printed Hydrogels, *Adv. Intell. Syst.*, 2022, **4**(1), 2100139.
8 K. Papadopoulos, E. Myrovali, D. Karfaridis, M. Farle, U. Wiedwald and M. Angelakeris, Cation substitution and size confinement effects on structure, magnetism and magnetic hyperthermia of $BiFeO_3$-based multiferroic nanoparticles and hydrogels, *J. Alloys Compd.*, 2023, **969**, 172337.
9 Z. Li, Y. Li, C. Chen and Y. Cheng, Magnetic-responsive hydrogels: From strategic design to biomedical applications, *J. Controlled Release*, 2021, **335**, 541–556.
10 R. Singh and B. Datta, Advances in Biomedical and Environmental Applications of Magnetic Hydrogels, *ACS Appl. Polym. Mater.*, 2023, **5**(7), 5474–5494.
11 J. Liao and H. Huang, Review on magnetic natural polymer constructed hydrogels as vehicles for drug delivery, *Biomacromolecules*, 2020, **21**(7), 2574–2594.
12 V. Pilati, G. Gomide, R. C. Gomes, G. F. Goya and J. Depeyrot, Colloidal stability and concentration effects on nanoparticle heat delivery for magnetic fluid hyperthermia, *Langmuir*, 2021, **37**(3), 1129–1140.
13 K. Büscher, C. A. Helm, C. Gross, G. Glöckl, E. Romanus and W. Weitschies, Nanoparticle composition of a ferrofluid and its effects on the magnetic properties, *Langmuir*, 2004, **20**(6), 2435–2444.
14 T. Yachi, M. Matsubara, C. Shen, S. Asami, N. B. Milbrandt, M. Ju, *et al.*, Water-Dispersible Fe_3O_4 Nanoparticles Modified with Controlled Numbers of Carboxyl Moieties for Magnetic Induction Heating, *ACS Appl. Nano Mater.*, 2021, **4**(7), 7395–7403.
15 H. Wu, L. Liu, L. Song, M. Ma, N. Gu and Y. Zhang, Enhanced tumor synergistic therapy by injectable magnetic hydrogel mediated generation of hyperthermia and highly toxic reactive oxygen species, *ACS Nano*, 2019, **13**(12), 14013–14023.
16 S. W. Ding, C. W. Wu, X. G. Yu, H. Li, L. Yu, Y. X. Zhang, R. P. Yang and W. Zhang, Magnetic hydrogel with long in situ retention time for self-regulating temperature hyperthermia, *Int. J. Hyperthermia*, 2021, **38**(1), 13–21.
17 M. Y. Naz, S. Shukrullah, A. Ghaffar, K. Ali and S. K. Sharma, Synthesis and processing of nanomaterials, in *Solar Cells: from materials to device technology*, 2020, pp. 1–23.
18 K. Papadopoulos, E. Myrovali, L. Malletzidou, D. Karfaridis, I. Tarasov, G. Vourliaset, *et al.*, Control of multiferroic features in $BiFeO_3$ nanoparticles by facile synthetic parameters, *Ceram. Int.*, 2023, **49**(11), 18552–18564.
19 H. M. Yusoff, M. N. Salimi and M. F. Jamlos, A review: Synthetic strategy control of magnetite nanoparticles production, *Adv. Nan. Res.*, 2018, **6**(1), 1.
20 K. Papadopoulos, E. Myrovali, A. Dubey, L. Malletzidou, D. C. Lupascu, V. V. Shvartsman, *et al.*, Control of physical properties in $BiFeO_3$ nanoparticles via Sm^{3+} and Co^{2+} ion doping, *Nanotechnology*, 2023, **35**(1), 015707.
21 E. Myrovali, K. Papadopoulos, I. Iglesias, M. Spasova, M. Farle, U. Wiedwald, *et al.*, Long-Range Ordering Effects in Magnetic Nanoparticles, *ACS Appl. Mater. Interfaces*, 2021, **13**(18), 21602–21612.
22 E. Myrovali, K. Papadopoulos, G. Charalampous, P. Kesapidou, G. Vourlias, T. Kehagias, *et al.*, Toward the separation of different heating mechanisms in magnetic particle hyperthermia, *ACS Omega*, 2023, **8**(14), 12955–12967.
23 J. Wang, Z. Peng, Y. Huang and Q. Chen, Growth of magnetite nanorods along its easy-magnetization axis of [1 1 0], *J. Cryst. Growth*, 2004, **263**(1–4), 616–619.
24 J. M. D. Coey, Noncollinear spin arrangement in ultrafine-ferrimagnetic crystallites, *Phys. Rev. Lett.*, 1971, **27**(17), 1140.
25 D. Fiorani, A. M. Testa, F. Lucari, F. D'orazio and H. Romero, Magnetic properties of maghemite nanoparticle systems: surface anisotropy and interparticle interaction effects, *Phys. B*, 2002, **320**(1–4), 122–126.
26 S. Jacob, A. B. Nair, V. Patel and J. Shah, 3D printing technologies: recent development and emerging applications in various drug delivery systems, *AAPS PharmSciTech*, 2020, **21**, 1–16.
27 R. C. R. Beck, P. S. Chaves, A. Goyanes, B. Vukosavljevic, A. Buanz, M. Windbergs, A. W. Basit and S. Gaisford, 3D printed tablets loaded with polymeric nanocapsules: An innovative approach to produce customized drug delivery systems, *Int. J. Pharm.*, 2017, **528**(1–2), 268–279.
28 D. Ukeba, H. Sudo, T. Tsujimoto, K. Ura, K. Yamada and N. Iwasaki, Bone marrow mesenchymal stem cells combined with ultra-purified alginate gel as a regenerative therapeutic strategy after discectomy for degenerated intervertebral discs, *EBioMedicine*, 2020, **53**, 102698.
29 P. Dorishetty, N. K. Dutta and N. R. Choudhury, Bioprintable tough hydrogels for tissue engineering applications, *Adv. Colloid Interface Sci.*, 2020, **281**, 102163.
30 P. E. Le Renard, O. Jordan, A. Faes, A. Petri-Fink, H. Hofmann, D. Ruefenacht, *et al.*, The in vivo performance of magnetic particle-loaded injectable, in situ gelling, carriers for the delivery of local hyperthermia, *Biomaterials*, 2010, **31**(4), 691–705.
31 Y. Zhang, J. Yu, K. Ren, J. Zuo, J. Ding and X. Chen, Thermosensitive hydrogels as scaffolds for cartilage tissue engineering, *Biomacromolecules*, 2019, **20**(4), 1478–1492.

32 J. Lai, X. Ye, J. Liu, C. Wang, J. Li, X. Wang, *et al.*, 4D printing of highly printable and shape morphing hydrogels composed of alginate and methylcellulose, *Mater. Des.*, 2021, **205**, 109699.
33 H. Zhang, X. Lin, X. Cao, Y. Wang, J. Wang and Y. Zhao, Developing natural polymers for skin wound healing, *Bioact. Mater.*, 2024, **33**, 355–376.
34 C. H. Goh, P. W. S. Heng and L. W. Chan, Alginates as a useful natural polymer for microencapsulation and therapeutic applications, *Carbohydr. Polym.*, 2012, **88**(1), 1–12.
35 F. L. Mi, H. W. Sung and S. S. Shyu, Drug release from chitosan–alginate complex beads reinforced by a naturally occurring cross-linking agent, *Carbohydr. Polym.*, 2002, **48**(1), 61–72.
36 P. Sriamornsak, N. Thirawong and K. Korkerd, Swelling, erosion and release behavior of alginate-based matrix tablets, *Eur. J. Pharm. Biopharm.*, 2007, **66**(3), 435–450.
37 M. Hamidi, A. Azadi and P. Rafiei, Hydrogel nanoparticles in drug delivery, *Adv. Drug Delivery Rev.*, 2008, **60**(15), 1638–1649.
38 K. Singla, M. Chawla and A. Singh, Potential applications of carbomer in oral mucoadhesive controlled drug delivery system: a review, *Drug Dev. Ind. Pharm.*, 2000, **26**(9), 913–924.
39 X. Du, N. Gao and X. Song, Bioadhesive polymer/lipid hybrid nanoparticles as oral delivery system of raloxifene with enhancive intestinal retention and bioavailability, *Drug Delivery*, 2021, **28**(1), 252–260.
40 B. Sun, R. Jia, H. Yang, X. Chen, K. Tan, Q. Deng, *et al.*, Magnetic Arthropod Millirobots Fabricated by 3D–Printed Hydrogels, *Adv. Intell. Syst.*, 2022, **4**(1), 2100139.
41 J. Liao and H. Huang, Review on magnetic natural polymer constructed hydrogels as vehicles for drug delivery, *Biomacromolecules*, 2020, **21**(7), 2574–2594.
42 N. F. Theodoroula, C. Karavasili, M. C. Vlasiou, A. Primikyri, C. Nicolaou, A. V. Chatzikonstantinouet, *et al.*, NGIWY-amide: a bioinspired ultrashort self-assembled peptide Gelator for local drug delivery applications, *Pharmaceutics*, 2022, **14**(1), 133.
43 C. Karavasili, D. A. Andreadis, O. L. Katsamenis, E. Panteris, P. Anastasiadou, Z. Kakazanis, *et al.*, Synergistic antitumor potency of a self-assembling peptide hydrogel for the local co-delivery of doxorubicin and curcumin in the treatment of head and neck cancer, *Mol. Pharm.*, 2019, **16**(6), 2326–2341.
44 E. Myrovali, Hybrid stents based on magnetic hydrogels for biomedical applications, *ACS Appl. Bio Mater.*, 2022, **5**(6), 2598–2607.
45 P. A. Amorim, M. A. d'Ávila, R. Anand, P. Moldenaers, P. Van Puyvelde and V. Bloemen, Insights on shear rheology of inks for extrusion-based 3D bioprinting, *Bioprinting*, 2021, **22**, e00129.
46 S. Ramesh, O. L. A. Harrysson, P. K. Rao, A. Tamayolet, D. R. Cormier, Y. Zhang, *et al.*, Extrusion bioprinting: Recent progress, challenges, and future opportunities, *Bioprinting*, 2021, **21**, e00116.
47 A. Schwab, R. Levato, M. D'Este, S. Piluso, D. Eglin and J. Malda, Printability and shape fidelity of bioinks in 3D bioprinting, *Chem. Rev.*, 2020, **120**(19), 11028–11055.
48 M. Barreiro Carpio, E. Gonzalez Martinez, M. Dabaghi, J. Ungureanu, A. V. Arizpe Tafoya, D. A. Gonzalez Martinez, J. A. Hirota, *et al.*, High-Fidelity Extrusion Bioprinting of Low-Printability Polymers Using Carbopol as a Rheology Modifier, *ACS Appl. Mater. Interfaces*, 2023, **15**(47), 54234–54248.
49 S. Jackson and T. Dickens, Rheological and structural characterization of 3D-printable polymer electrolyte inks, *Polym. Test.*, 2021, **104**, 107377.
50 M. Zhou, B. H. Lee, Y. J. Tan and L. P. Tan, Microbial transglutaminase induced controlled crosslinking of gelatin methacryloyl to tailor rheological properties for 3D printing, *Biofabrication*, 2019, **11**(2), 025011.
51 S. Koltsakidis, V. Koidi, A. Lappas, E. Heracleous and D. Tzetzis, Influence of binder concentration in zeolitic ZSM-5/bentonite 3D-printed monoliths manufactured through robocasting for catalytic applications, *Int. J. Adv. Des. Manuf. Technol.*, 2023, **126**(1), 259–271.
52 T. Chatzitaki, M. Patila, S. Haralampos, I. S. Vizirianakis, E. A. Rekka, D. Tzetziset, *et al.*, Development of mucoadhesive 3D-printed Carbopol/Eudragit/SNAC tablets for the oral delivery of enoxaparin: In vitro and ex vivo evaluation, *Int. J. Pharm.*, 2024, **664**, 124627.
53 S. Mallakpour, M. Tukhani and C. M. Hussain, Recent advancements in 3D bioprinting technology of carboxymethyl cellulose-based hydrogels: Utilization in tissue engineering, *Adv. Colloid Interface Sci.*, 2021, **292**, 102415.
54 S. Yamashita, M. Kataoka, H. Higashino, S. Sakuma, T. Sakamoto, H. Uchimaru, H. Tsukikawa, *et al.*, Measurement of drug concentration in the stomach after intragastric administration of drug solution to healthy volunteers: analysis of intragastric fluid dynamics and drug absorption, *Pharm. Res.*, 2013, **30**, 951–958.
55 T. Y. Liu, S. H. Hu, T. Y. Liu, D. M. Liu and S. Y. Chen, Magnetic-sensitive behavior of intelligent ferrogels for controlled release of drug, *Langmuir*, 2006, **22**(14), 5974–5978.
56 Z. Wang, C. Liu, B. Chen and Y. Luo, Magnetically-driven drug and cell on demand release system using 3D printed alginate based hollow fiber scaffolds, *Int. J. Biol. Macromol.*, 2021, **168**, 38–45.
57 C. A. Cezar, S. M. Kennedy, M. Mehta, J. C. Weaver, L. Gu, H. Vandenburgh and D. J. Mooney, Biphasic ferrogels for triggered drug and cell delivery, *Adv. Healthcare Mater.*, 2014, **3**(11), 1869–1876.